IMAGE REGISTRATION USING AN EXTENDABLE QUADRATIC REGULARISER

A. Melbourne[1]*, N. D. Cahill*[2]*, C. Tanner*[1]*, D. J. Hawkes*[1]

[1]Centre for Medical Image Computing, University College London, UK,
[2]School of Mathematical Sciences, Rochester Institute of Technology, NY, USA.

ABSTRACT

Image registration algorithms are widely used in medical imaging to spatially align anatomical features. This work investigates the regularisation of the registration transformation by unification of the standard diffusion equation regulariser with the standard curvature regulariser. A variational non-rigid registration scheme is employed with periodic boundary conditions and tested over a range of regularisation parameters. A variable regularisation algorithm is also proposed that automatically adapts the regularisation as the registration progresses. Improved registration performance on two simulated biomechanical deformations of 3D breast MRI over four subjects is observed; correcting the simulated deformation residual by 69% and 73% respectively for diffusion regularisation, 36% and 45% for curvature regularisation and up to 73% and 75% for variable regularisation.

***Index Terms*—** registration, regularisation, diffusion, breast MRI

1. INTRODUCTION

Image registration algorithms are commonly used throughout medical imaging for the alignment of features in two images. Accurate alignment of features allows a quantitative comparison of the images and the transformations between them that can improve both diagnostic and therapeutic assessment. A large number of publications address the issue of non-rigid image registration, with wide ranging applications such as oncology and neuroscience. A particular application is the investigation of breast cancer and the comparison of 2D projection X-ray data with 3D volumetric MRI in order to correlate findings on both modalities. This comparison is aided if the large deformations between the two modalities can be modelled or estimated using biomechanical modelling or image registration [1]. Automatic image registration algorithms typically optimise a correspondence by maximising a measure of image similarity. Since the image similarity measure generally does not contain information about a position's neighbours a constrained solution can be guaranteed using a regularisation term: neighbouring regions of an image are aligned with a similar deformation (obeying traditional notions of locality and causality). The use of the calculus of variation is common in regularisation methods such as optical flow and when invoking partial differential equations for solving diffusion or elastic equations [2] [3].

A general image registration algorithm acts to minimise a cost function such as the example in (1), assuming a metric of image similarity d_S between two images A and B, combined with a distance of the transformation d_R from some ideal set of transformations. An explicit example for the sum-of-squared difference image similarity measure and an *l2-norm* regularisation penalty for a smooth deformation field $\mathbf{u}$ is given in (2) over the region of image overlap Ω. This cost-function is typically minimised using the calculus of variation seeking displacements $\mathbf{u}$ for which $\nabla d_T = 0$ resulting in a partial differential equation (PDE) (3). This representation is typically described as diffusion-based registration and is closely related to optical-flow algorithms [4].

$$d_T = d_S(A, B(\mathbf{u})) + d_R(\mathbf{u}) \quad (1)$$

$$= \int_\Omega (A - B(\mathbf{u}))^2 + ||\nabla \mathbf{u}||_2^2 d\Omega \quad (2)$$

$$\nabla^2 \mathbf{u} = (A - B(\mathbf{u}))\nabla B(\mathbf{u}) \quad (3)$$

The PDE in (3) can be solved rapidly using discrete Fourier transform techniques for a range of boundary conditions [5]. A similar method can be applied to the solution of the curvature equation where d_R in (2) is given by: $||\nabla^2 \mathbf{u}||_2^2$. This work uses the results of the Fourier transform solution to the PDE's to propose a method of interpolating between the diffusion and curvature regularisers, applied to non-rigid image registration, to generate a novel framework for variational multi-resolution PDE based registration.

2. METHOD

The method proceeds by analysing the results of the diffusion and curvature equations. In the case of diffusion we are looking for a solution for the velocity field $\mathbf{v}$ of $\nabla^2 \mathbf{v} = \mathbf{F}(A, B(\mathbf{u}))$, where $\mathbf{F}$ is the local force generated by minimising the sum of squared differences (SSD) in the first term in (2). The velocity field is used to update the applied deformation field, $\mathbf{u}$, using a forward finite difference in time. This is subtly different from (2) since we are applying the diffusion equation to the velocity field to enable us to accommodate

larger deformations. The SSD will be used throughout this work since it is appropriate for the simulated data used, where each image is registered to the same image transformed by the known biomechanical deformation with a low level of visible image intensity noise. Both the force field $\mathbf{F}$ and the resulting velocity field $\mathbf{v}$ can be represented as linear combinations of eigenfunctions ϕ_k of the discrete diffusion operator $\hat{\nabla}^2$ such that $\mathbf{v} = \sum_k c_k \phi_k$ and $\mathbf{F} = \sum_k d_k \phi_k$. This form of the discrete Laplacian operator (4) results in expressions (5, 6) for the diffusion and curvature regularisers respectively.

$$\hat{\nabla}^2 \phi_k(j) = \phi_k(j-1) + \phi_k(j+1) - 2\phi_k(j) \quad (4)$$

$$\hat{\nabla}^2 \phi_k = \omega_k \phi_k \quad (5)$$

$$\hat{\nabla}^2 (\hat{\nabla}^2) \phi_k = \omega_k^2 \phi_k \quad (6)$$

The eigenfunctions used in this work are chosen to maintain periodic boundary conditions and are thus represented by complex exponentials. For the 3D case we may write the eigenfunctions as (7). In this case the corresponding eigenvalues are found to be given by (8).

$$\phi_k = \beta \prod_{d=1}^{3} \exp\left(\frac{2ik_d j_d \pi}{N_d}\right) \quad (7)$$

$$\omega_k = \sum_{d=1}^{3} \left[2\cos\frac{2k_d\pi}{N_d} - 2\right] \quad (8)$$

We now generalise the solution via an interpolation of the results for the diffusion and curvature equation using the approximation in (9) for continuous α which meets the correspondence principle for the diffusion equation for $\alpha = 1$, the curvature equation for $\alpha = 2$ and no regularisation for $\alpha = 0$.

$$\hat{\nabla}^{2\alpha} \phi_k \approx \omega_k^{\alpha} \phi_k \quad (9)$$

The solution of (9) over the linear basis of an arbitrary velocity field can be found using a fast-Fourier technique [5] for periodic boundary conditions making use of the Fourier transform Ψ (11). An update scheme for large deformations can then be applied to find the deformation field $\mathbf{u}$ from the instantaneous velocity field $\mathbf{v}$ (12) via a forward difference in time and we may loop steps (10-12) until convergence.

$$\mathbf{F}^t = (B(\mathbf{u}^t) - A)\nabla B(\mathbf{u}^t) \quad (10)$$

$$\mathbf{v}_x = \Psi^{-1}(\Psi(\mathbf{F}_x^t)/|\omega^{\alpha}|) \quad (11)$$

$$\mathbf{u}^{t+1} = \mathbf{u}^t + \Delta t\left(\mathbf{v} - \mathbf{v}\cdot\nabla\mathbf{u}^t\right) \quad (12)$$

It should be noted that the solution of (11) changes sign between the diffusion and curvature operators. For this reason we ensure a consistent direction to the solution by taking the magnitude of the corresponding eigenvalues. The resulting velocity field is then normalised by the maximum gradient magnitude in order to compare results for different α.

The fundamental problem now is a correct choice of α. The value of α is representative of how smoothed the final velocity field is, so the choice is dependent on the images in question and their initial registration state. We start by contemplating the situation that the images are poorly aligned, thus a highly smoothed deformation might be expected to provide a good initial alignment. Subsequent iterations are likely to refine the alignment so greater flexibility in the transformation can be tailored by using more local regularisation. We use these assumptions to justify varying α during the registration via (13) or (14): the value of α is initialised to 2 and reduces as the registration progresses and the image similarity improves. $\alpha \to 1$ as SSD $\to 0$, so the driving forces are never unregularised and the algorithm moves from curvature regularisation towards the lower limit of diffusion regularisation. In principle there is no reason for limiting $1 \leq \alpha \leq 2$ (we show results for fixed α: $0.6 \leq \alpha \leq 2$), however we limit our work to this range to investigate the behaviour of (9) between the two standard quadratic regularisers. Without a good reason to prefer either (13) or (14) we proceed to use both; (13) will have a faster fall off from global to local regularisation as the SSD reduces during registration.

$$\alpha(t) = \frac{\sum_n (A_n - B_n(\mathbf{u}^t))^2}{\sum_n (A_n - B_n(\mathbf{u}^0))^2} + 1 \quad (13)$$

$$\alpha(t) = \left[\frac{\sum_n (A_n - B_n(\mathbf{u}^t))^2}{\sum_n (A_n - B_n(\mathbf{u}^0))^2}\right]^{\frac{1}{2}} + 1 \quad (14)$$

2.1. Data

The proposed algorithm is tested on simulated deformations applied to three-dimensional MR mammography. Simulated deformations applied to four cases are generated by the application of a finite element model of breast deformation to MRI data using the method and four breast volumes from Guy's Hospital, UK [6] . Deformations are modelled over two force types to simulate differences due to a range of common breast imaging deformations. Two force types are modelled: a simulations of twin plate-like compressions (TP); and simulation of pectoral muscle movement from tension to relaxation (PR). Biomechanical deformations are applied at a maximum displacement magnitude of $10mm$. Each biomechanical simulation $\mathbf{u}_{sim}$ is applied to an undeformed image B to produce a fixed image A (thus, $A = B(\mathbf{u}_{sim})$). A low-level of Rician noise is also added to the deformed images and images are resampled using cubic interpolation. We can now use the residual: $||\mathbf{u}_{sim} - \mathbf{u}_{reg}||_2^2$ with the final registration transformation, $\mathbf{u}_{reg}$, averaged over all displacement vectors as a measure of assessment. Registrations are carried out in 3D.

3. RESULTS

In addition to varying α, the registration algorithm is tested over a range of fixed $0.6 < \alpha \leq 2$ to check that the algorithm is robust and visually convergence is well-behaved and monotonic. The range of α is chosen to encompass values of inter-

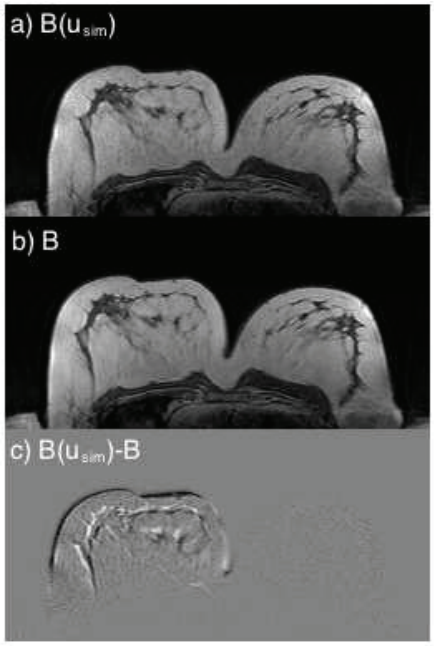

Fig. 1. Example slice from a deformed MR volume subject to the $10mm$ TP simulation. a) undeformed slice B; b) deformed slice $B(\mathbf{u}_{sim})$ and c) difference image $B(\mathbf{u}_{sim}) - B$. A small amount of Rician noise is added prior to deformation.

est between the standard diffusion and curvature regularisers; values of $\alpha < 1$ are found to be progressively poorer at registration. In addition, we investigate the effect of varying α on the final image similarity, final deformation residual and the algorithm convergence properties. Registrations terminate if the SSD metric no longer reduces or after 150 iterations, a criteria that is found to be sufficient for these results.

Figure 2 shows results for four subjects under the TP and PR simulations for $10mm$ displacement magnitude. The deformation field residual between the applied deformation and the registration deformation is shown for a range of values of α. The pre-registration residual value is marked on the left and results for the variable α algorithms (13,14) are shown to the far right. The registration status of the images is improved for all tested values of α with minima in the range $1 \leq \alpha \leq 1.2$. For each biomechanical simulation, the residual is improved by 69% and 73% for TP and PR respectively for diffusion regularisation and 36% and 45% for curvature regularisation, averaged over the four subjects. The lowest residual value is found for $\alpha = 1.1$ at 71% and 73% for each simulation. The results for the variable α schemes in (13,14) respectively reduce the residual by 73% & 75% and 62% & 69%: thus the scheme in (13) appears to show a performance benefit over fixed regularisation. Discrepancies in the results are visibly associated with the alignment of detailed regions of fibroglandular tissue rather than the breast boundary.

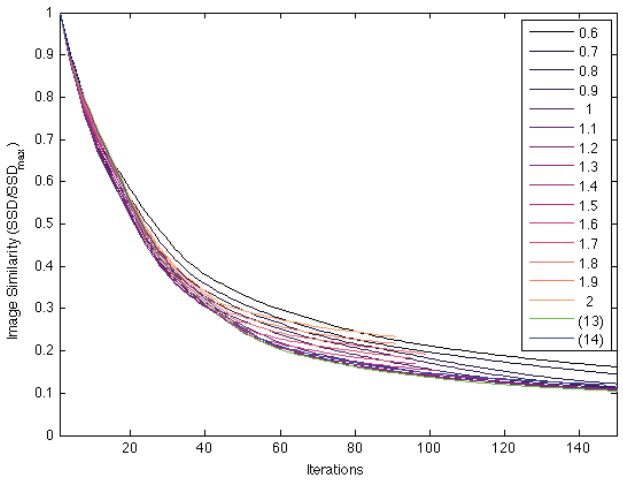

Fig. 3. Convergence behaviour for a single subject under the TP simulation for a range of α and variable α (13) and (14). Registration terminates earlier for more global regularisation (larger α). The final SSD values for each α correlate well with the residuals marked as S1 in figure 2a.

Figure 3 shows the registration convergence behaviour for the sum-of-squared difference cost-function for the range of α discussed above. For the simulation shown (TP), convergence is smooth and monotonic over a range of comparable trajectories. For more global regularisation, the registration algorithm terminates early; this is due to the increased limitation on the flexibility of the registration transformation. However, the initial convergence is more rapid due to the propagation of larger forces with more global regularisation. Also shown is the convergence behaviour for the variable α schemes, (13,14) respectively: these registrations take an intermediate trajectory, converging across the fixed α curves as might be expected. However, by the final few iterations the scheme in (13), isabel to reduce the image similarity further, implying that the earlier transformations carried out at large α allow improved registration at a later stage.

4. CONCLUSION

This work has developed a method for extending the quadratic family of image registration regularisers used in medical image registration. Increasing the range and flexibility of the regularisation term has shown the potential for improvements in registration performance, which in combination with other multi-resolution strategies could be extremely effective. Interestingly for the data shown here, absolute registration minima are often found between the limiting values of the diffusion ($\alpha = 1$) and curvature ($\alpha = 2$) regularisers. An adaptive regularisation is shown to increase the accuracy of the registration of simulated breast MRI deformations, combining

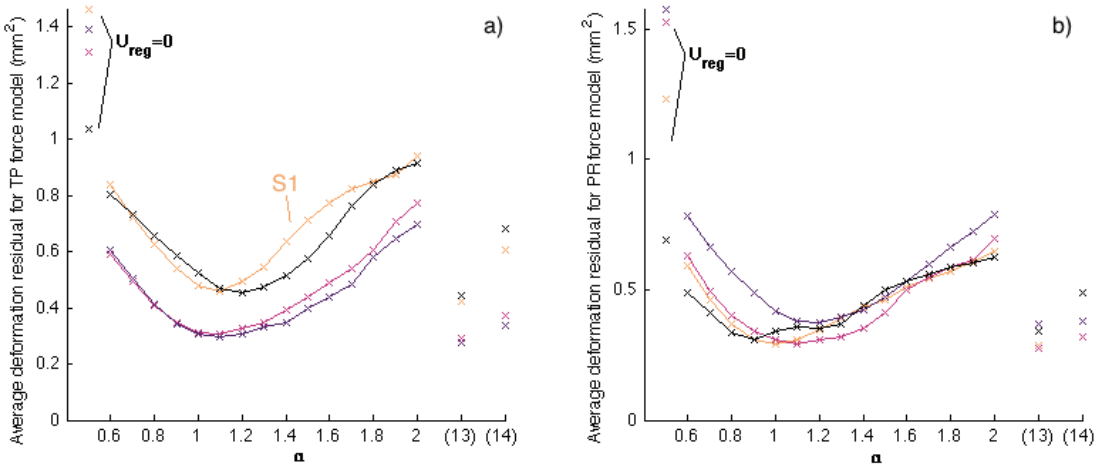

Fig. 2. Changes to the registration residual $||\mathbf{u}_{sim} - \mathbf{u}_{reg}||_2^2$ for a range of values of α for four subjects over two force models. a) *twin-plate compression* force model (TP) (for S1 label see figure 3), b) *pectoral muscle tension* force model (PR). The labelled left most data-points are the residual values prior to registration ($\mathbf{u}_{reg} = 0$); right most data-points correspond to results for variable α schemes (13) and (14) respectively.

rapid initial convergence with ultimately more accurate registration under more local regularisation. The adaptive regularisation method implemented in this work is related, although certainly not identical to, a multi-resolution approach and could be compared to a recursive kernel smoothing approach [2]. A further comparison of algorithms could investigate differences in performance when applying the diffusion regulariser over subsampled driving image forces from (10); however, the solution shown here is independent of sampling choice and generates a smooth family of regularisers that is elegant even if found to be practically unnecessary.

The mechanism for varying the value of α may be extended to many other image similarity measures, providing they are easily normalised to a suitable range. The value of α may also be chosen by inspecting the deformation transformation during the registration, for instance by adapting the regularisation to the maximum applied displacement. The authors intend to extend this method to a wider range of values of α (it may be advantageous to allow more local regularisation for $\alpha < 1$ as the optimal transformation is reached) and apply the method on real deformation data beyond the relatively simple deformations used in this work. It is also conceivable to extend the eigenvalue interpolation method to the elastic and 2^{nd}-order elastic PDE's used as image registration regularisers. In conclusion, this work has developed a novel extension to a common family of image registration regularisers that could be of wider interest.

Acknowledgements

This work was funded by the European 7th Framework Program, HAMAM, ICT-2007.5.3 and EPSRC grant EP/E031579/1.

5. REFERENCES

[1] Timothy Carter, Christine Tanner, Nicolas Beechey-Newman, Dean Barratt, and David Hawkes, "Mr navigated breast surgery: method and initial clinical experience.," *Med Image Comput Comput Assist Interv*, vol. 11, pp. 356–363, 2008.

[2] J. P. Thirion, "Image matching as a diffusion process: an analogy with Maxwell's demons.," *Medical Image Analysis*, vol. 2, no. 3, pp. 243–260, 1998.

[3] Bernd Fischer and Jan Modersitzki, "Curvature based image registration," *Journal of Mathematical Imaging and Vision*, vol. 18, pp. 81:85, 2003.

[4] Berthold K.P. Horn and Brian G. Schunck, "Determining optical flow," *Artificial Intelligence*, vol. 17, pp. 185–203, 1981.

[5] Nathan D. Cahill, J. Alison Noble, and David J. Hawkes, "Fourier methods for nonparametric image registration," in *Computer Vision and Pattern Recognition*, 2007.

[6] Christine Tanner, Julia A Schnabel, Derek L G Hill, David J Hawkes, Andreas Degenhard, Martin O Leach, D. Rodney Hose, Margaret A Hall-Craggs, and Sasha I Usiskin, "Quantitative evaluation of free-form deformation registration for dynamic contrast-enhanced MR mammography.," *Medical Physics*, vol. 34, no. 4, pp. 1221–1233, 2007.